Optical properties and sensing in plexcitonic nanocavities: from simple molecular linkers to molecular aggregate layers

2014 Nanotechnology 25 035201

(http://iopscience.iop.org/0957-4484/25/3/035201)

IOP Publishing Nanotechnology

Nanotechnology **25** (2014) 035201 (6pp) doi:10.1088/0957-4484/25/3/035201

Optical properties and sensing in plexcitonic nanocavities: from simple molecular linkers to molecular aggregate layers

Olalla Pérez-González[1,2], Nerea Zabala[1,2] and Javier Aizpurua[2]

[1] Department of Electricity and Electronics, University of the Basque Country UPV/EHU, 48080 Bilbao, Spain
[2] Donostia International Physics Center (DIPC) and Centro de Física de Materiales, Centro Mixto CSIC-UPV/EHU, Paseo Manuel Lardizabal 4, 20018 Donostia/San Sebastián, Spain

E-mail: nerea.zabala@ehu.es

Received 8 October 2013
Accepted for publication 30 October 2013
Published 17 December 2013

Abstract

We present a theoretical study of a metal–molecular aggregate hybrid system consisting of a strongly coupled dimer connected by molecules characterized by an excitonic transition. The plasmonic resonances of the metallic dimer interact with the molecular excitations giving rise to coupled plasmon–exciton states, so called plexcitons. We compare the differences in the optical response when the excitonic material is placed only as a linker in the plasmonic gap of the dimer and when the material is distributed as an aggregate layer covering the dimer entirely. We also explore the efficiency of plexcitons for localized surface plamon resonance (LSPR) sensing in both situations. The ordinary shift-based sensing is more efficient for dimers connected through molecular linkers, whereas intensity-based sensing is more effective when the molecular aggregate covers the entire nanostructure. These results can serve to design the chemistry of excitons around metallic nanoparticles.

Keywords: plasmonics, molecular aggregates, sensing

(Some figures may appear in colour only in the online journal)

1. Introduction

In recent years plasmonics [1, 2] has played an important role in nanotechnology due to its applications in biosensing, surface-enhanced spectroscopies, cancer therapies, renewable energies or active devices [3–7]. Among the great variety of structures considered, plasmonic dimers have emerged as a useful canonical nanostructure to understand basic plasmonic processes. The bonding dimer plasmon (BDP) mode, arising from the hybridization of the dipolar modes of the individual nanoparticles (NPs) of the dimer, presents a huge enhancement of the near-field in the gap, known as the hot-spot [4]. This mode is the main localized surface plamon resonance (LSPR) governing the optical response of nearly touching dimers [8, 9]. In contrast, when a conductive path between both NPs is established, a charge transfer plasmon (CTP) mode is allowed, in which the whole nanostructure behaves as a dipole, and an oscillating distribution of net charge at every individual NP is involved [9]. Since nowadays well-defined molecular conductance can be measured as standard in circuits made of single molecules [10–12], the possibilities of molecular linkers, to establish conductive paths and also to understand their role in the optical properties of the entire molecule-plasmonic electrodes system, have been intensively studied [13–16]. In parallel, there has been a growing interest in the interaction between plasmonic systems and excitons (in i.e. quantum dots) with potential applications in active devices [7, 17–20]. When a quantum

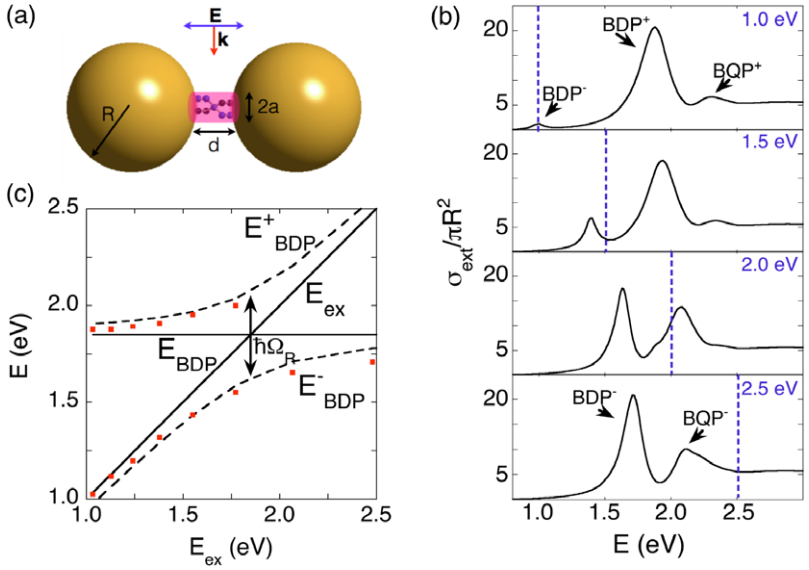

Figure 1. (a) Schematic representation of a gold NP dimer connected by a molecular linker modelled as a cylinder of radius a and length d. The radius of the gold NPs is $R = 50$ nm and the minimum separation distance between them is $d = 1$ nm (proportionality is not to scale in this sketch). **k** is the wavevector of the incident electromagnetic plane wave with polarization of the electric field **E** along the vertical symmetry axis of the system. (b) Calculated normalized optical extinction cross-section of a gold nanoparticle dimer bridged by a molecular linker, with length $d = 1$ nm and fixed radius $a = 5$ nm, as the energy of the exciton is varied; the reduced oscillator strength of the molecular transition is $f = 0.5$ and the damping is $\gamma = 0.1$ eV. The vertical blue dashed lines indicate the excitation energy E_{ex} considered in each panel. (c) Anti-crossing behaviour of the BDP^+ and BDP^- plexciton modes. The superimposed red squares indicate the spectral position of the plexciton modes calculated for the system in (a), whereas the dashed lines indicate the theoretical energies of the BDP^+ plexciton (E^+_{BDP}) and the BDP^- (E^-_{BDP}) derived from equation (2).

dot or emitter is placed in the surroundings of a metallic nanostructure, excitons, consisting of electron–hole pairs created by the absorption of photons, couple to the LSPRs giving rise to plasmon–exciton states [21–24]. Although the plasmon–exciton coupling is an inherently quantum process, many of its properties have been described within classical electrodynamics [25, 26].

In this paper we present a theoretical study of the optical properties of a hybrid plasmonic nanostructure which consists of a strongly coupled gold NP dimer–molecular aggregate system, which extends previous work where a single molecular linker had been considered [25]. The molecular aggregate is characterized by the presence of an excitonic transition which substantially alters the behaviour of the LSPRs of the dimer. The plasmon cavity modes, the BDP and the bonding quadrupolar plasmon (BQP, which arises from the hybridization of the quadrupolar modes of the individual NPs), couple to the excitons in the molecular aggregate, giving rise to plasmon–exciton states named plexcitons. In this work we consider a molecular shell that covers both NPs. We then explore the optical response in relation to the energy of the optical excitonic transition and the efficiency for sensing in the cases of pristine and aggregate-covered dimers.

2. Plexcitons in molecular linkers

The nanostructure under study (see figure 1(a)) is a gold NP dimer, where the radius of each NP is $R = 50$ nm, and the separation distance between them is $d = 1$ nm. The interparticle distance is short enough so that the system is strongly coupled and, consequently, the LSPRs are easy to trace. However, this distance is above the critical value for quantum effects, such as tunnelling, to emerge [27]. We first consider that the molecular aggregate is a linker filling the interparticle gap, modelled as a cylindrical junction of length equal to the interparticle gap d, radius a, and top and bottom endings matching properly the spherical geometry of the nanostructure.

The gold NPs are characterized by an experimental dielectric function from the literature [28], whereas the molecular linker is characterized by means of a Drude–Lorentz model. All the molecules in the linker are assumed to be identical in this model and characterized by a single molecular transition of energy $E_{ex} = \hbar\omega_{ex}$, so that their dielectric response as a function of frequency $\varepsilon_l(\omega)$ can be described as [29]

$$\varepsilon_l(\omega) = 1 - \frac{f\omega_{ex}^2}{(\omega^2 - \omega_{ex}^2) + i\omega\gamma_{ex}}, \qquad (1)$$

where γ_{ex} is the damping, related to the lifetime of the electronic excitation, and f is the reduced oscillator strength, a dimensionless magnitude related to the density of electrons in the junction participating in the transition. In this manner, the imaginary part of the dielectric function presents a Lorentzian shape that results in a resonant behaviour of the conductance through the molecular linker [25].

In order to explore the optical response of the system, we solve Maxwell's equations in the presence of the inhomogeneous media using the boundary element method (BEM) to obtain the electromagnetic fields and the optical extinction cross-section of the entire system [30]. Local

dielectric functions, already introduced, are used to describe the response of the materials in these calculations. Results are analysed in terms of extinction cross-sections and near-field plots.

It is well known in atomic physics that the presence of an atom or a molecule produces the splitting of the resonances in an optical cavity [31–33]. Similarly, in our system, the cavity BDP and BQP resonances couple to the excitons in the molecular linker, giving rise to plexcitons [25]. The resulting mixed BDP–exciton modes are the BDP^+ and BDP^- modes, while the BQP^+ and BQP^- modes arise from the BQP–exciton coupling. Within this notation, the + and − signs refer to higher and lower energies, respectively. The original spectral positions of the BDP and BQP modes of the considered dimer when there is no linker filling the interparticle gap are $E_{BDP} = 1.86$ eV ($\lambda_{BDP} = 665$ nm) and $E_{BQP} = 2.30$ eV ($\lambda_{BQP} = 540$ nm). Figure 1(b) shows the calculated normalized optical extinction cross-section of a gold NP dimer bridged by a molecular linker of radius $a = 5$ nm as the energy characterizing the optical transition in the cavity E_{ex} is varied. The reduced oscillator strength of the molecular transition is $f = 0.5$ and the damping $\gamma = 0.1$ eV. The nature of the resulting resonances has been analysed in terms of the symmetry of the near-field patterns calculated for each branch (not shown here [34]). We observe that the BDP mode clearly splits into two branches, the BDP^+ and BDP^- plexcitons. The BQP cavity mode, which also splits into two plexcitons, BQP^- and BQP^+ [25], is a minor spectral feature that is not easy to trace in this case. For the lowest excitonic energy shown here, $E_{ex} = 1.0$ eV (top panel), the low-energy BDP^- and the high-energy BQP^+ plexcitons can be distinguished, the high-energy BDP^+ plexciton being the main spectral feature. As E_{ex} is increased, the BDP^- blue-shifts towards higher energies (but always lower than the pure excitonic transition given by the dashed lines), becoming the predominant mode. In parallel, both the BDP^+ and BQP^+ slightly blue-shift while increasingly losing intensity. For the highest transition energy considered, $E_{ex} = 2.5$ eV (bottom panel), the low-energy BDP^- plexciton is the main mode, while the BQP^- mode, negligible for lower excitation energies, also emerges. As the excitation energy is increased, the BDP^+ becomes more influenced by the $BQP^\pm$ plexcitons due to the small spectral distance between them in this particular geometry.

This coupling of the plasmon cavity modes to the excitons in the plasmonic cavity can be interpreted in terms of a simple model of two coupled oscillators [24–26, 35]. According to this coupled-oscillator model, the energies of the plexciton modes can be described by [24, 33]

$$E^{\pm} = \frac{E_P + E_{ex}}{2} \pm \left[\left(\frac{\hbar\Omega_R}{2} \right)^2 + \frac{1}{4}(E_P - E_{ex})^2 \right]^{1/2}, \quad (2)$$

where E_P and E_{ex} are the energies of the LSPRs (BDP or BQP) and the exciton, respectively. The term $\hbar\Omega_R$ is the Rabi splitting [31, 32], which is obtained from the full electrodynamical calculations when $E_P = E_{ex}$. For the BDP mode, the Rabi splitting is found to be $\hbar\Omega_R \approx 440$ meV. Figure 1(c) shows the anti-crossing behaviour of the BDP^+ and BDP^- plexcitons centred in the point of intersection of the exciton and BDP energy lines. The dashed lines represent the theoretical prediction for the energies $E^\pm$ of the $BDP^\pm$ plexcitons given by equation (2), while the superimposed red squares correspond to the spectral position of the $BDP^\pm$ plexcitons in figure 1(b), obtained from the electrodynamical calculation. A good agreement between the prediction of the simple model and the electrodynamical simulation is observed.

3. Plexcitons in molecular aggregates

In practice, molecular aggregates usually adopt the form of layers that cover plasmonic nanostructures [7, 21–24]. It is therefore natural to extend our study and consider that the molecular aggregate, previously regarded as a linker filling the plasmonic cavity between the NPs forming the dimer, actually covers the whole dimer, forming a spherical shell which surrounds the NPs. Figure 2 shows the comparison between the optical response of the gold NPs when the molecular linker is placed only inside the gap separating the NPs and when it covers the whole nanostructure. The molecular aggregate cover is modelled as a spherical shell of width $w = 1$ nm equal to the interparticle distance, and with the same linker previously described in equation (1) filling the interparticle gap. As a reference, in figure 2(a) the calculated normalized optical extinction cross-section of the uncovered dimer is also represented ($R = 50$ nm, $d = 1$ nm and $a = 10$ nm), as the energy of the exciton is varied. In the contour plot, we clearly observe the splitting of the BDP and BQP modes into plexcitons and their evolution as the transition energy is varied. The BDP mode, originally found at $E_{BDP} = 1.86$ eV ($\lambda_{BDP} = 665$ nm) when there is no linker bridging the gap, splits into two plexciton modes, the BDP^+ plexciton, with higher energy than the BDP, and the BDP^- plexciton, with lower energy than the BDP. The near-field patterns, not shown here, show a clear dipole–dipole structure with large field enhancement in the gap or hot-spot [4]. The same behaviour is observed for the BQP mode, which splits into the BQP^+ and BQP^-, even though this is a minor spectral feature, less easy to trace. In this case, even though a conductive path through the dimer is established, we do not observe the emergence of the charge transfer plasmon (CTP) mode, arising from the hybridization of the monopolar modes of the individual NPs [9, 14, 15]. The concept of conductance threshold was previously introduced for conductive junctions [14, 15], but was shown to be still valid for excitonic linkers [25]. With the particular parameters of our geometry and the value of the reduced oscillator strength $f = 0.5$ used here, the conductance through the linker ($G_{max} \approx 159G_0$) is below the threshold value $G_{CTP} \approx 672G_0$ that indicates the necessary conductance for the CTP mode to emerge.

Complementary to figures 2(a) and (b) shows the calculated normalized optical extinction cross-section of a gold NP dimer entirely covered by a molecular aggregate layer of width $w = 1$ nm with the same excitonic material as in figure 2(a). In this case, the splitting of the BDP and BQP

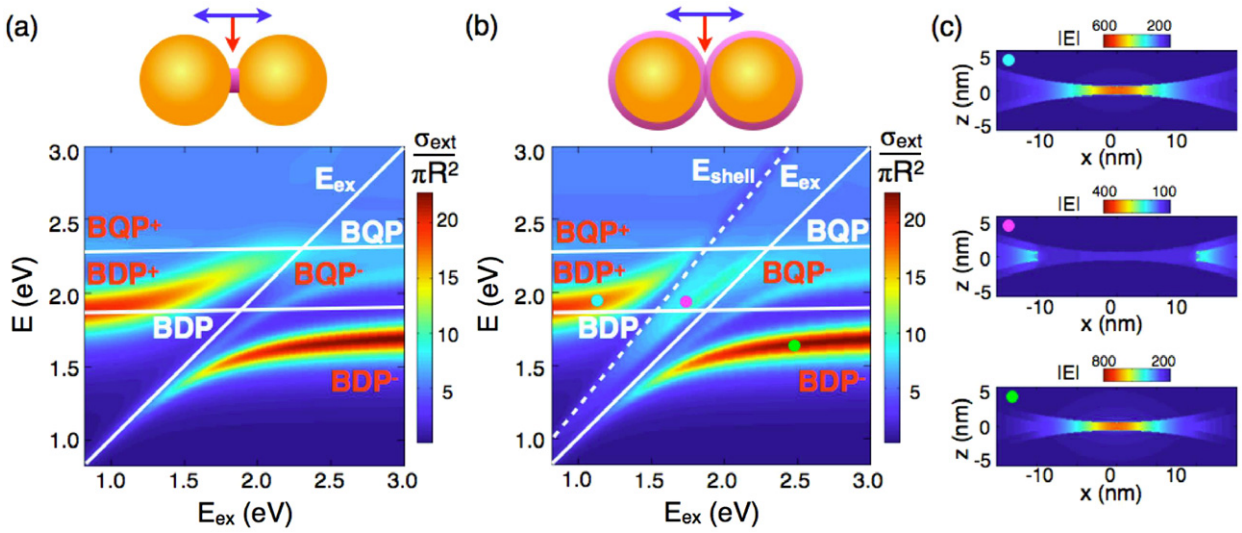

Figure 2. (a) Calculated normalized optical extinction cross-section of a gold NP dimer bridged by a molecular linker, with length $d = 1$ nm and fixed radius $a = 10$ nm, as the energy of the exciton is varied. The reduced oscillator strength of the molecular transition is kept constant $f = 0.5$. The white solid line indicates the energy of the exciton. (b) Calculated normalized optical extinction cross-section of a gold NP dimer covered by a molecular aggregate layer of width $w = 1$ nm as the energy of the exciton is varied. The reduced oscillator strength of the molecular transition is constant $f = 0.5$. The interparticle distance d and the radius of the linker in the gap a are the same as in (a). The white solid line indicates the energy of the exciton, whereas the white dashed line indicates the energy line of the excitonic shell. (c) Near-field plots at the interparticle gap region corresponding to the spectral regions marked in (b) by coloured dots.

modes into the $BDP^{\pm}$ and $BQP^{\pm}$ plexcitons is also clearly observed. The low-energy BDP^{-} and BQP^{-} plexcitons are barely altered by the presence of the molecular layer, exactly as the extremely weak BQP^{+} mode. In contrast, the BDP^{+} plexciton, which remains unaltered for low excitation energies, becomes altered by the presence of the molecular aggregate shell as E_{ex} is increased. Indeed, a new resonance can be observed in the centre of the contour plot, when $E > E_{ex}$, which cuts the tail of the BDP^{+} plexciton (magenta dot). This new resonance arises from the interaction between the plasmon cavity modes and the geometrical modes of the molecular aggregate in the molecular shell, given by the white dashed line in figure 2(b). We identify this effect by calculating the normalized optical extinction cross-section of the molecular aggregate shell–dimer without gold inside that shows the presence of two peaks: the most intense one corresponding to the excitonic transition in bulk (indicated by the E_{ex} energy line in figure 2(b)), and a less intense one (indicated by the E_{shell} dashed line in figure 2(b)) that becomes weaker as E_{ex} is decreased and corresponds to the geometrical mode of the excitonic shell. Last, figure 2(c) shows the near-field patterns at the interparticle gap of the entirely covered nanostructure corresponding to the coloured dots marked in figure 2(b). In the top and bottom panels we notice the hot spots with a large field enhancement corresponding respectively to BDP^{+} (cyan point, $E_{ex} = 1.24$ eV; $\lambda_{ex} = 1240$ nm, $E = 1.91$ eV; $\lambda = 650$ nm) and BDP^{-} (green point, $E_{ex} = 2.48$ eV; $\lambda_{ex} = 500$ nm, $E = 1.64$ eV; $\lambda = 755$ nm) modes. The central panel shows the near-field at the interparticle gap for the shell-resonance (magenta point, $E_{ex} = 1.77$ eV; $\lambda_{ex} = 700$ nm, $E = 1.91$ eV; $\lambda = 650$ nm), where the field is expelled from the gap, still remaining concentrated mainly around the plasmonic cavity.

4. Sensing in plexcitonic aggregates

The use of plasmonic structures as sensors has become one of the main potential applications of plasmonics [2]. LSPR sensing is based on the detection of spectral changes of LSPRs due to variations of the dielectric environment. In this section, we compare the possibilities of plexcitons for LSPR sensing in our geometry. Figure 3(a) shows the calculated normalized optical extinction cross-section of the uncovered gold NP dimer as the dielectric constant of the embedding medium ε_d is varied for exciton energy $E_{ex} = 1.24$ eV ($\lambda_{ex} = 1000$ nm), whereas figure 3(b) shows the analogous case for the NP dimer entirely covered with the same type of molecular aggregate as used for the linker in (a). The behaviours of the BDP^{+} and BDP^{-} differ as the dielectric constant ε_d of the medium embedding the nanostructure is varied. The spectral position of the BDP^{+} plexciton mode is red-shifted towards longer wavelength values as ε_d is increased (see figure 3(a)), which is the ordinary trend of LSPRs. The efficiency of plasmonic systems as sensors in shift-based LSPR sensing is usually estimated by the figure of merit (FOM), which is defined as [36]

$$\mathrm{FOM} = m(\mathrm{eV}/RIU)/fwhm(\mathrm{eV}). \tag{3}$$

In this expression m is the linear regression slope for the refractive index dependence, which indicates the ratio of the plasmon energy shift to the change in refractive index of the embedding medium, and *fwhm* is the full width at half maximum of the mode. From the results shown in figures 3(a) and (b), we obtain FOM = 2.5 for the BDP^{+} plexciton of the bridged nanostructure, and FOM = 1.2 for the BDP^{+} of the entirely covered nanostructure. These values suggest that the NP dimer connected by a molecular linker is more efficient for

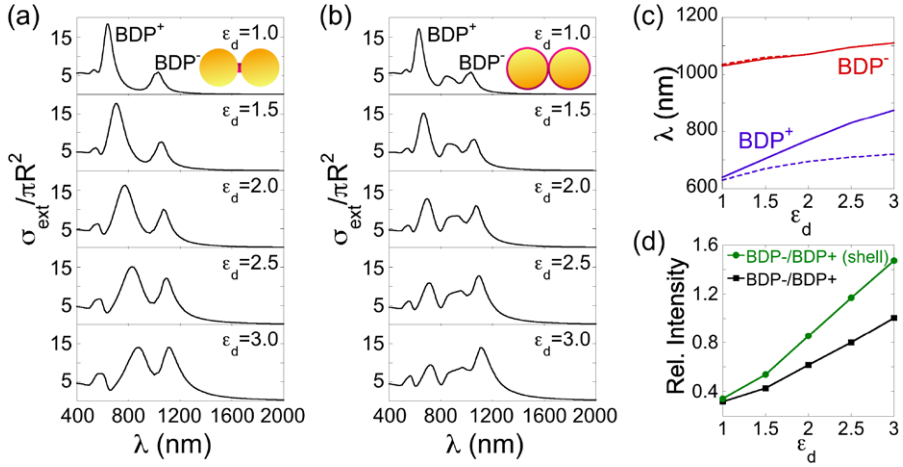

Figure 3. (a) Calculated normalized optical extinction cross-section of a gold NP dimer bridged by a molecular linker, with length $d = 1$ nm and fixed radius $a = 10$ nm, exciton energy $E_{ex} = 1.24$ eV ($\lambda_{ex} = 1000$ nm) and reduced oscillator strength $f = 0.5$, as the dielectric constant of the embedding medium is varied. (b) Calculated normalized optical extinction cross-section of a gold NP dimer covered by a molecular aggregate layer, of width $w = 1$ nm, and the material in the gap used in (a), as the dielectric constant of the embedding medium is varied. (c) Shift of the BDP^+ and BDP^- modes in (a) and (b) as a function of the dielectric constant of the embedding medium. (d) Variation of the relative intensity of the BDP^-/BDP^+ modes in (a) and (b) as a function of the dielectric constant of the embedding medium.

sensing than the dimer with the molecular aggregate covering the whole nanostructure. This is due to the appearance of the shell-resonance which blocks the red-shift of the BDP^+ (see solid (linker) and dashed (shell) blue lines in figure 3(c)).

The behaviour of the BDP^- is quite different when increasing ε_d. In both cases (the molecular linker and the molecular layer), the BDP^- hardly red-shifts and shows an unconventional behaviour (see red lines in figure 3(c)). This plexciton, which is a minor spectral feature when the embedding medium is vacuum, hardly red-shifts as the surrounding dielectric constant ε_d is increased. However, by increasing ε_d the BDP^- mode becomes as strong as the BDP^+ mode in terms of intensity (for the molecular linker), or even stronger (for the molecular layer), as shown in figure 3(d), where the relative intensities of the BDP^+ and BDP^- modes are traced as the embedding dielectric constant ε_d is varied. This figure shows that, for large values of the dielectric constant, the BDP^- mode gains enough spectral weight, becoming more intense than the BDP^+, indicating that the balance of spectral weight of both plexcitons can be inverted by means of a change in the dielectric embedding medium. We believe that this dramatic variation of the relative intensity of the lower energy plexciton mode might be the key for a strategy of LSPR sensing based on the variation of the intensity of the peaks rather than on their shift. This behaviour had already been introduced in [25], but we now observe that it can be improved by considering a full molecular layer that screens the intensity of the BDP^+ mode, thus favouring the change in the relative intensity between the BDP^+ and BDP^- plexcitons.

The different behaviour of the BDP^+ and BDP^- plexciton modes can be easily understood with the help of figures 2(a) and 2(b). The BDP^+ mode at the cross-sections for excitation energy $E_{ex} = 1.24$ eV presents a plasmon-like behaviour, thus red-shifting as the dielectric constant of the embedding medium is increased (as plasmon resonances do in standard LSPR sensing). In contrast, the BDP^- plexciton presents an excitonic-like character, thus keeping its energy constant as the medium is varied. This suggests that, depending on the purpose of the sensing, plexciton modes can be tuned by means of the excitation energy E_{ex} to exhibit a more or less pronounced exciton/plasmon-like behaviour. In our case, we also observe that this intensity-based sensing can be exploited more efficiently when the molecular aggregate covers the whole NP dimer compared to the situation where it is placed only in the interparticle cavity.

5. Conclusions

In conclusion, we have studied theoretically the optical properties of a plasmonic cavity consisting of a strongly coupled metallic dimer when an ensemble of molecules, characterized by an excitonic transition, entirely covers the nanostructure. The bonding dimer plasmon (BDP) and the bonding quadrupolar plasmon (BQP) resonances couple to the excitonic transition, splitting into two coupled plasmon–exciton modes, called plexcitons. In comparison to the case when the molecules are placed only in the interparticle gap, for the entirely covered dimer a new resonance emerges, arising from the interaction of the plasmon cavity modes and the geometrical modes of the molecular aggregate layer. We have also analysed the efficiency of the new mixed states for LSPR sensing, showing that the plexcitons emerging from the BDP–exciton coupling present an interesting behaviour for sensing based on the change of the relative intensity of the resonances. This effect is more evident when the nanostructure is entirely covered by a molecular layer. This introduces a new framework for sensing based on the evolution of plexcitonic intensities rather than on spectral shifts for molecular layers sited on plasmonic antennas.

Acknowledgments

This project was supported by the Etortek project Nanoiker from the Basque Government (BG), project FIS2010-19609-C02-01 from the Spanish Ministry of Science and Innovation and grant IT-75613 from BG-UPV/EHU. OPG acknowledges financial support from Vicerrectorado de Investigación of the University of the Basque Country (Ayudas Especialización Doctores). Computational resources were provided by DIPC (UPV/EHU, MICINN, BG, ESF).

References

[1] Pelton M, Aizpurua J and Bryant G W 2008 *Laser Photon. Rev.* **2** 136
[2] Halas N J, Lal S, Chang W S, Link S and Nordlander P 2011 *Chem. Rev.* **111** 3913
[3] McFarland A D and Van Duyne R P 2003 *Nano Lett.* **3** 1057
[4] Xu H, Aizpurua J, Käll M and Apell P 2000 *Phys. Rev.* E **62** 4318
[5] Choi M R *et al* 2007 *Nano Lett.* **7** 3759
[6] Atwater H and Polman A 2010 *Nature Mater.* **9** 205
[7] Zheng Y B, Yang Y, Jensen L, Fang L, Juluri B K, Flood A H, Weiss P S, Stoddart J F and Huang T J 2009 *Nano Lett.* **9** 819
[8] Nordlander P, Oubre C, Prodan E, Li K and Stockman M I 2004 *Nano Lett.* **4** 899
[9] Romero I, Aizpurua J, García de Abajo F J and Bryant G W 2006 *Opt. Express* **14** 9988
[10] Reed M A, Zhou C, Muller C J, Burgin T P and Tour J M 1997 *Science* **278** 252
[11] Xiao X, Xu B and Tao N J 2004 *Nano Lett.* **4** 267
[12] Venkataraman L, Klare J E, Tam I W, Nuckolls C, Hybertsen M S and Steigerwald M L 2006 *Nano Lett.* **6** 458
[13] Ward D R, Halas N J, Ciszek J W, Tour J M, Wu Y, Nordlander P and Natelson D 2008 *Nano Lett.* **8** 919
[14] Pérez-González O, Zabala N, Borisov A G, Halas N J, Nordlander P and Aizpurua J 2010 *Nano Lett.* **10** 3090
[15] Pérez-González O, Zabala N and Aizpurua J 2011 *New J. Phys.* **13** 083013
[16] Alber I, Sigle W, Demming-Janssen F, Neumann R, Trautmann C, van Aken P A and Toimil-Molares M E 2012 *ACS Nano* **6** 9711
[17] Artuso R D and Bryant G W 2008 *Nano Lett.* **8** 2106
[18] Artuso R D, Bryant G W, García-Etxarri A and Aizpurua J 2011 *Phys. Rev.* B **83** 235406
[19] Manjavacas A, García de Abajo F J and Nordlander P 2011 *Nano Lett.* **11** 2318
[20] Singh M R 2013 *Nanotechnology* **24** 125701
[21] Bellessa J, Bonnand C, Plenet J C and Mugnier J 2004 *Phys. Rev. Lett.* **93** 036404
[22] Wurtz G A, Evans P R, Hendren W, Atkinson R, Dyckson W, Pollard R J and Zayats A V 2007 *Nano Lett.* **7** 1297
[23] Fofang N T, Park T, Neumann O, Mirin N A, Nordlander P and Halas N J 2008 *Nano Lett.* **8** 3481
[24] Gómez D E, Vernon K C, Mulvaney P and Davis T J 2010 *Nano Lett.* **10** 274
[25] Pérez-González O, Aizpurua J and Zabala N 2013 *Opt. Express* **21** 15847
[26] Schlather A E, Large N, Urban A S, Nordlander P and Halas N J 2013 *Nano Lett.* **13** 3281
[27] Esteban R, Borisov A G, Nordlander P and Aizpurua J 2012 *Nature Commun.* **3** 825
[28] Johnson P B and Christy R W 1972 *Phys. Rev.* B **6** 4370
[29] Dressel M and Grüner G 2002 *Electrodynamics of Solids* (Cambridge: Cambridge University Press) p 139
[30] García de Abajo F J and Howie A 2002 *Phys. Rev.* B **65** 115418
[31] Sánchez-Mondragón J J, Naroznhy N B and Eberly J H 1983 *Phys. Rev. Lett.* **51** 550
[32] Agarwal G S 1984 *Phys. Rev. Lett.* **53** 1732
[33] Rudin S and Reinecke T L 1999 *Phys. Rev.* B **59** 10227
[34] Zabala N, Pérez-González O, Nordlander P and Aizpurua J 2011 *Proc. SPIE* **8096** 80961L
[35] Wu X, Gray S K and Pelton M 2010 *Opt. Express* **18** 23633
[36] Sherry L J, Chang S H, Schatz G C and Van Duyne R P 2005 *Nano Lett.* **5** 2034